Photon polarization in the ^{4}He($\gamma,\vec{d}$)^{2}H reaction

Edward L. Tomusiak
Department of Physics and Engineering Physics and Saskatchewan Accelerator Laboratory, University of Saskatchewan, Saskatoon, Canada S7N 0W0

Winfried Leidemann
Dipartimento di Fisica, Università di Trento, I-38050 Povo (Trento), Italy

Hartmut M. Hofmann
Institut für Theoretische Physik, Universität Erlangen-Nürnberg, Erlangen, Germany
(Received 12 April 1995)

We derive double polarization observables for the photodisintegration of ^{4}He with an incident polarized photon beam. In particular we study the effect of the ground state α-particle D wave on these observables in a simple nuclear model. We find that in general the double polarization observables offer no clear advantage to the corresponding variables studied in the single polarization ^{4}He($\gamma,\vec{d}$)^{2}H reaction. However, the photon asymmetry Σ appears as a promising observable for the study of ground state effects.

PACS number(s): 24.70.+s, 25.10.+s, 25.20.Dc, 27.10.+h

I. INTRODUCTION

The process of photodisintegration of the α particle has been studied for decades. Despite the fact that it is a light nucleus, the photodisintegration process is complicated by the presence of five open channels when the γ ray energy is above about 27 MeV. The dominant decay channels are the $E1$-driven ^{3}He-n and ^{3}H-p channels while a much weaker, but to some extent more interesting decay channel is the isoscalar, dominantly $E2$-driven d-d channel. Recent interest in this channel has focused on the possibility of obtaining information on the D state of the ^{4}He ground state from either photodisintegration or capture experiments. It was, in fact, low-energy capture experiments which demonstrated conclusively the presence of this nonspherical component of the α particle. One of the earliest theoretical studies of this process dates back to the 1951 paper of Flowers and Mandl [3]. A review of the field up to 1988 is given by Weller and Lehman [4].

A source of difficulty has been the interpretation of experiments in the relative void of well-founded theoretical calculations. In the case of the very low ($\approx$75 keV) capture experiments of Refs. [1,2] the interpretation was rather clear; namely, capture had to proceed mainly through the continuum (L=0, S=2, J=2) state to the (L=2, S=2, J=0) component of the ground state or else the rate would be down by orders of magnitude. This was a strong argument for the presence of the D component. However, to say anything more quantitative required better theoretical input. For example, Piekarewicz and Koonin [5] have shown that one has also to consider $E2$ radiation coming from (022) $\rightarrow$(000) transitions which are mediated through the quadrupole moment of the deuteron. In their model the capture cross section arises from a delicate destructive interference between the (022)$\rightarrow$(220) and the (022)$\rightarrow$(000) amplitudes. Depending on whether one considered this channel or not one could arrive at disparate values of the D-wave parameters such as the percentage of D state or asymptotic D/S ratio. In addition, the work of Blüge, Assenbaum, and Langanke [6] demonstrated that it is essentially impossible to extract reliable information on the ^{4}He ground state by using simple potential models of structureless deuterons to describe the capture reaction. The most ambitious theoretical treatment so far is the multichannel resonating group calculation of Wachter, Mertelmeier, and Hofmann [7] in which four channels, ^{3}He-n, ^{3}H-p, d-d, and d-$d\!\!\!/$, are coupled. Here $d\!\!\!/$ is a singlet deuteron to mock up the d-np channel. However, that work did not consider D-wave components in any of the fragments and so, based on the warning from Ref. [5], the authors considered it premature to draw conclusions about the D state admixture in ^{4}He. Later Arriaga, Pandharipande, and Schiavilla [22] performed a variational calculation based on the Argonne V14 potential which did include D waves in both the α particle and the deuterons. However, this work did not include coupling to the ^{3}He-n and ^{3}H-p channels. Their results did not agree with the data but indicated, as in [5], that the deuteron D state does make an important contribution to the low-energy capture reaction.

The paragraph above describes difficulties in using very low-energy ($<$100 keV) d-d capture cross sections to extract details about the D component in ^{4}He. Another series of experiments using polarized deuterium beams at $E_{\mathrm{c.m.}}\geqslant$ 5 MeV was instigated by Weller and collaborators [8–11] and by Mellema, Wang, and Haeberli [12,13]. The use of polarized deuterons enabled the various vector and tensor analyzing powers to be measured. Angular distributions clearly indicated the dominance of $E2$ radiation and attempts were made to extract the D-state percentage by adjusting simple models to fit the data. However, again here it was found [12] that even though $E2$ radiation is dominant the presence of

0556-2813/95/52(4)/1963(9)/$06.00

other multipoles could radically alter D-state parameters extracted on the basis of assuming only $E2$ multipoles. Subsequently Tostevin [14] employed a single channel model which included $M1$, $E1$, $M2$, and $E2$ radiation and utilized other theoretical input to estimate various overlap integrals and initial state distortions. He was able to give a reasonable account of the $E_{\text{c.m.}}=5$ MeV data for A_y and A_{yy}. However, this model gave a serious underprediction of T_{20} and Tostevin concluded that the $(022)\rightarrow(220)$ amplitude was poorly described in his model thereby indicating the need for an actual microscopic calculation. Such a calculation, as mentioned above, was carried out in Ref. [7] and was able to give a good account of both the 5 MeV data and the data on the astrophysical S factor. However, the agreement is not as good, especially for the polarization observables, with the new 10, 15, and 25 MeV data published by Whitton *et al.* [11]. As stated in Ref. [11] this may be due to a combination of effects resulting from the use of a semirealistic NN potential, the neglect of deuteron D waves, and partial wave truncation.

The polarization observables discussed in the capture experiments, namely, A_{yy}, T_{20}, and especially A_y are very sensitive to fine details of the wave functions and to small admixtures of multipole radiation. This is especially so as the energy increases. Thus it is possible that this sensitivity may render it nearly impossible to learn about specifics such as the D-state details. That is as yet unclear. There are, however, other polarization observables which have not as yet been studied which may be more suitable for studying specific effects. For this reason we consider in this paper a range of polarization observables accessible in the photodisintegration process. Besides the observables for unpolarized radiation, which are the same as those previously studied in d-d capture experiments, we look in particular at the differential cross section and polarization observables resulting from a polarized incident photon beam. Such experiments should be feasible at facilities which can produce high-intensity polarized photon beams

In this work we want to set out the formalism and the definition of the various observables and, furthermore, assess their suitability by means of a simple nuclear model. It will also allow us to check the importance of higher electromagnetic multipole transitions ($E3$, $M3$, $E4$, $M4$). Such a study is important with regard to the resonating group calculation of [7] or other realistic calculations, where the evaluation of higher multipoles requires an enormous numerical effort.

II. FORMALISM

The theoretical description of reactions involving photons and polarized nuclei has been treated by a number of authors in the past. The work by Seyler and Weller [15] considers unpolarized radiation and polarized reactants. It addition it contains references to much of the earlier work on the topic including the general treatment by Welton [16]. Here we want to consider the combined possibilities of using polarized radiation as well as polarized deuterons in the treatment of the $^4\text{He}(\vec{\gamma},\vec{d})^2\text{H}$ reaction or its time reversed capture counterpart. For this reason we present our own formalism, not for the case of arbitrary targets and projectiles as in Refs. [15,16], but for the $^4\text{He}(\vec{\gamma},\vec{d})^2\text{H}$ reaction. Since we now have a spin-0 target (or final nucleus) there naturally is a substantial simplification in the formulas. While the expressions for the double polarization observables are given for the first time we have checked our results for the single polarization observables against the more general formulas found in the literature.

We discuss our results for the photodisintegration process. The modifications to these results which would allow their use in the capture process will be described at the end of this section. Taking the detected deuteron direction $\hat{\kappa}$ as the quantization axis we use the deuteron density matrix

$$(\rho_d)_{m',m}=\frac{1}{3}\sum_{I,M} T^*_{IM}\hat{I}C^{1\ I\ 1}_{m\,M\,m'} \tag{1}$$

and the photon density matrix[1]

$$(\rho_\gamma)_{\lambda',\lambda}=\tfrac{1}{2}[\delta_{\lambda',\lambda}+P_l\delta_{\lambda',-\lambda}+P_c\lambda\,\delta_{\lambda',\lambda}]. \tag{2}$$

Here P_l is the linear polarization (P_y-P_x). Note that for a spin-zero target there is no contribution from circular photon polarization P_c, regardless of the polarization state of the outgoing deuterons. Thus we henceforth omit this term in the photon density matrix. The photodisintegration cross section leading to a tensor polarization T_{IM} of the detected deuteron in the c.m. system is given by

$$\frac{d\sigma}{d\Omega}\langle T_{IM}\rangle=\sigma_0[f_{IM}(\theta,\phi)+P_l f'_{IM}(\theta,\phi)] \tag{3}$$

where

$$\sigma_0=4\pi\alpha\left(\frac{\kappa}{q}\right)\frac{M_dc^2}{\hbar c}\frac{1}{1+\dfrac{\hbar cq}{M_\alpha c^2}}. \tag{4}$$

In the above equation the structure functions corresponding to polarized and unpolarized incident radiation are given by

$$f_{IM}=\langle\tau_{IM}\rangle_{1,1}, \tag{5}$$

$$f'_{IM}=\tfrac{1}{2}[\langle\tau_{IM}\rangle_{1,-1}+\langle\tau_{IM}\rangle_{-1,1}], \tag{6}$$

where

[1]Here a caret over a scalar quantity, e.g., $\hat{L}$, stands for $\sqrt{2L+1}$, while over a vector quantity, e.g., $\hat{\mathbf{q}}$, it represents a unit vector.

$$\langle \tau_{IM}\rangle_{\lambda',\lambda}=(-1)^{1+I}\sqrt{3}\hat{I}\sum_{k,k_l}\sum_{JLSJ'L'S'}\hat{k}_l\hat{L}\hat{L}'\hat{S}\hat{S}'\hat{J}\hat{J}'(-1)^{L'+S'+J'}[i]^{J-J'-L+L'}C^{LL'k_l}_{00\ 0}C^{JJ'\ \ k}_{\lambda-\lambda'\lambda-\lambda'}C^{k_lI\ k}_{0\ MM}\begin{Bmatrix} S' & 1 & 1\\ 1 & I & S\end{Bmatrix}$$
$$\times\begin{Bmatrix} L & S & J\\ L' & S' & J'\\ k_l & I & k\end{Bmatrix}D^{(k)}_{M,\lambda-\lambda'}\langle JLS||(T^{\rm el}_J+\lambda T^{\rm mag}_J)||i\rangle\langle J'L'S'||(T^{\rm el}_{J'}+\lambda' T^{\rm mag}_{J'})||i\rangle^*. \tag{7}$$

Here we use reduced matrix elements as defined by Edmonds [17], and electromagnetic multipole operators as defined by deForest and Walecka [18]. The D matrix arises from the rotation which takes the system where the photon momentum $\hat{\mathbf{q}}$ is the z axis into the system where $\hat{\kappa}$ is the z axis. There are no factors of i absorbed into spherical harmonics or state vectors as is often done to give nicer looking results under time reversal. We denote the photon and relative d-d wave numbers by q and κ, respectively. The angular dependence of the $\langle \tau_{IM}\rangle_{\lambda',\lambda}$ can be made more explicit by writing

$$\langle \tau_{IM}\rangle_{\lambda',\lambda}=\sum_k A_{\lambda',\lambda}(IM,k)d^{(k)}_{M,\lambda-\lambda'}(\theta)e^{i\phi(\lambda-\lambda'-M)} \tag{8}$$

where

$$A_{\lambda',\lambda}(IM,k)=\sum_{k_l} C^{k_l\ I\ k}_{0\ \ MM}F(k,k_l,\lambda',\lambda;IM) \tag{9}$$

and where

$$F(k,k_l,\lambda',\lambda;IM)=(-1)^{I+1}\sqrt{3}\hat{I}\hat{k}_l\sum_{JLSJ'L'S'}\hat{L}\hat{L}'\hat{S}\hat{S}'\hat{J}\hat{J}'(-1)^{L'+S'+J'}[i]^{J-J'-L+L'}$$
$$\times C^{LL'k_l}_{00\ 0}C^{JJ'\ \ k}_{\lambda-\lambda'\lambda-\lambda'}\begin{Bmatrix} S' & 1 & 1\\ 1 & I & S\end{Bmatrix}\begin{Bmatrix} L & S & J\\ L' & S' & J'\\ k_l & I & k\end{Bmatrix}$$
$$\times\langle JLS||(T^{\rm el}_J+\lambda T^{\rm mag}_J)||i\rangle\langle J'L'S'||(T^{\rm el}_{J'}+\lambda' T^{\rm mag}_{J'})||i\rangle^*. \tag{10}$$

For unpolarized radiation, i.e., $\lambda=\lambda'$, the variables k and k_l can be shown to satisfy $k+k_l$=even, while for $\lambda\neq\lambda'$ that condition only holds for $M=0$. One can also show that the $A_{\lambda',\lambda}(IM,k)$ have the following symmetry properties (note that λ and λ' are restricted to the values ± 1):

$$A_{\lambda',\lambda}(IM,k)=(-1)^I A_{-\lambda',-\lambda}(I-M,k) \tag{11}$$

$$=A^*_{\lambda,\lambda'}(I-M,k), \tag{12}$$

$$A_{\lambda,\lambda}(IM,k)=A_{-\lambda,-\lambda}(IM,k), \tag{13}$$

and that T_{IM} indeed has the spherical tensor property that $T^*_{IM}=(-1)^M T_{I-M}$. In addition these formulas say that the A's are real for I=0 or 2 and pure imaginary for I=1. Finally they guarantee the vanishing of $A_{\lambda,\lambda}(10,k)$ and any contribution from circular photon polarization.

Equation (3) gives the tensor polarization components of the outgoing deuteron. It is useful to rewrite this equation directly in terms of physical observables $P_{\mathcal{O}}$ which can be taken as [19]

$$P_z=\sqrt{\frac{2}{3}}T_{10}, \tag{14}$$

$$P_{x/y}=\frac{\delta_{nx}+i\,\delta_{ny}}{\sqrt{3}}(T_{1-1}\mp T_{11}),\quad n=x,y, \tag{15}$$

$$P_{zz}=\sqrt{2}T_{20}, \tag{16}$$

$$P_{xx/yy}=\pm\frac{\sqrt{3}}{2}(T_{22}+T_{2-2})-\frac{1}{\sqrt{2}}T_{20}, \tag{17}$$

$$P_{xy}=i\,\frac{\sqrt{3}}{2}(T_{2-2}-T_{22}), \tag{18}$$

$$P_{x/yz}=(\delta_{nx}+i\,\delta_{ny})\frac{\sqrt{3}}{2}(T_{2-1}\mp T_{21}), \tag{19}$$

with $P_n=\langle S_n\rangle$, while the tensor components P_{mn} are defined as

$$P_{mn}=\tfrac{3}{2}\langle S_mS_n+S_nS_m\rangle-2\,\delta_{mn},\quad m,n=x,y,z. \tag{20}$$

We note that the condition $A_{\lambda,\lambda}(10,k)=0$ gives $P_z=0$. Differential cross sections for nonpolarized deuterons are given by

$$\frac{d\sigma}{d\Omega}=\sigma_0[f_{00}(\theta)+P_l\, f'_{00}(\theta,\phi)]$$

$$=\sigma_0\sum_k\, [A_{1,1}(00,k)d^{(k)}_{0,0}+P_lA_{1,-1}(00,k)d^{(k)}_{0,2}\cos(2\phi)]$$

$$=\sigma_0 f_{00}[1+P_l\Sigma(\theta)\cos(2\phi)] \tag{21}$$

where Σ is the photon asymmetry. With deuteron polarization the cross sections for the various polarization observables are given by

$$\frac{d\sigma}{d\Omega}\,P_{\angle}=\sigma_0 f_{00}[p_{\angle}+P_lp'_{\angle}] \tag{22}$$

with

$$p_{\angle}=\frac{\pi_{\angle}}{f_{00}},\quad p'_{\angle}=\frac{\pi'_{\angle}}{f_{00}}, \tag{23}$$

and where

$$\pi'_z=\sqrt{\frac{2}{3}}\sum_k\, \mathrm{Im}[A_{1,-1}(10,k)]d^{(k)}_{0,2}\sin(2\phi), \tag{24}$$

$$\pi_{x/y}=-\frac{2}{\sqrt{3}}\sum_k\, \mathrm{Im}[A_{1,1}(11,k)]d^{(k)}_{1,0}\sin/\cos(\phi), \tag{25}$$

$$\pi'_{x/y}=\mp\frac{1}{\sqrt{3}}\sum_k\, [\mathrm{Im}[A_{1,-1}(1-1,k)]d^{(k)}_{1,2}\sin/\cos(\phi)$$

$$\pm\mathrm{Im}[A_{1,-1}(11,k)]d^{(k)}_{1,-2}\sin/\cos(3\phi)], \tag{26}$$

$$\pi_{zz}=\sqrt{2}\sum_k\, A_{1,1}(20,k)d^{(k)}_{0,0}, \tag{27}$$

$$\pi'_{zz}=\sqrt{2}\sum_k\, A_{1,-1}(20,k)d^{(k)}_{0,2}\cos(2\phi), \tag{28}$$

$$\pi_{xx/yy}=\pm\sqrt{3}\sum_k\, A_{1,1}(22,k)d^{(k)}_{2,0}\cos(2\phi)-\frac{1}{2}\,\pi_{zz}, \tag{29}$$

$$\pi'_{xx/yy}=\pm\frac{\sqrt{3}}{2}\sum_k\, [A_{1,-1}(2-2,k)d^{(k)}_{2,2}$$

$$+A_{1,-1}(22,k)d^{(k)}_{2,-2}\cos(4\phi)]-\frac{1}{2}\,\pi'_{zz}, \tag{30}$$

$$\pi_{x/yz}=\mp\sqrt{3}\sum_k\, A_{1,1}(21,k)d^{(k)}_{1,0}\cos/\sin(\phi), \tag{31}$$

$$\pi'_{x/yz}=-\frac{\sqrt{3}}{2}\sum_k\, [A_{1,-1}(2-1,k)d^{(k)}_{1,2}\cos/\sin(\phi)$$

$$\pm A_{1,-1}(21,k)d^{(k)}_{1,-2}\cos/\sin(3\phi)], \tag{32}$$

$$\pi_{xy}=-\sqrt{3}\sum_k\, A_{1,1}(22,k)d^{(k)}_{2,0}\sin(2\phi), \tag{33}$$

$$\pi'_{xy}=-\frac{\sqrt{3}}{2}\sum_k\, A_{1,-1}(22,k)d^{(k)}_{2,-2}\sin(4\phi). \tag{34}$$

In the above equations all functions $A_{\lambda',\lambda}(IM,k)$ are real except those where the imaginary part has been taken, in which case they are purely imaginary. The observables $p_{\angle}$ and $p'_{\angle}$ are bounded by $(-1,1)$ for vector observables, by $(-2,1)$ for p_{mm} and p'_{mm} observables, and by $(-3/2,3/2)$ for p_{nm} and p'_{nm} $(m\neq n)$ tensor observables. The photon asymmetry Σ ranges from -1 to $+1$.

Finally we give the form of the differential cross section for the case of $\vec{d}$-d capture in the c.m. system. For the case of unpolarized outgoing radiation one has

$$\frac{d\sigma}{d\Omega}=\alpha\,\frac{8\pi}{9}\left(\frac{q}{\kappa}\right)\frac{M_dc^2}{\hbar c}\,\frac{1}{1+\dfrac{\hbar cq}{M_\alpha c^2}}\sum_{I,M}\,T^*_{IM}\langle\tau_{IM}\rangle_{1,1}, \tag{35}$$

while the angular distribution of radiation with linear polarization is given by

$$\frac{d\sigma}{d\Omega}\,P_l=\alpha\,\frac{8\pi}{9}\left(\frac{q}{\kappa}\right)\frac{M_dc^2}{\hbar c}\,\frac{1}{1+\dfrac{\hbar cq}{M_\alpha c^2}}\sum_{I,M}\,T^*_{IM}\frac{1}{2}[\langle\tau_{IM}\rangle_{1,-1}$$

$$+\langle\tau_{IM}\rangle_{-1,1}]. \tag{36}$$

Here T_{IM} are the polarization components of the target deuteron and the $\langle\tau_{IM}\rangle_{\lambda,\lambda'}$ are given by Eq. (7). For the case discussed by Seyler and Weller, namely, unpolarized radiation with $\phi=0$, the above formulas agree with theirs.

III. DESCRIPTION OF THE MODEL

We use a number of phenomenological Saxon-Woods potentials, i.e.,

$$V(r)=\frac{V_0}{1+\exp[(r-c)/a_0]}, \tag{37}$$

which have been used by others to describe the deuteron-deuteron interaction. Parameters for the bound state potentials are taken from Piekarewicz and Koonin [5], while those for the continuum state are from Weller [20]. The ground state is thus a completely phenomenological mixture

$$\Psi=\cos(\alpha)\psi_S+\sin(\alpha)\psi_D \tag{38}$$

where the angle α controls the amount of D wave. Table I summarizes the values of the parameters. In addition we also use a free wave in the final state to indicate the sensitivity of the results to final state interactions.

Reduced matrix elements of the multipole operators are easily obtained in this model. Since we are dealing with an isoscalar transition the usual isovector two-body exchange currents do not contribute. Thus, neglecting the small isoscalar two-body currents, we take the current operator as that given by

TABLE I. Saxon-Woods potential parameters.

	Partial-wave quantum numbers	V_0 (MeV)	c (fm)	a_0 (fm)
Bound	$L=S=0$	−74.00	1.70	0.90
	$L=S=2$	−191.50	1.70	0.90
Continuum	$S=0,\ J=L=2$	−13.5	3.39	0.79
	$S=1,\ J=L=1$	−13.5	5.04	0.79
	$S=2,\ J=2,\ L=0,2,4$	−15.5	3.59	0.81

$$\hat{\mathbf{J}}(\mathbf{x})=\hat{\mathbf{j}}(\mathbf{x})+\nabla_{\mathbf{x}}\times\hat{\mu}(\mathbf{x}), \tag{39}$$

where the convection and magnetization parts are taken as

$$\hat{\mathbf{j}}(\mathbf{x})=\frac{1}{2m_d}[\hat{\mathbf{p}}_1\delta^3(\mathbf{x}-\mathbf{r}_1)+\delta^3(\mathbf{x}-\mathbf{r}_1)\hat{\mathbf{p}}_1+\hat{\mathbf{p}}_2\delta^3(\mathbf{x}-\mathbf{r}_2)+\delta^3(\mathbf{x}-\mathbf{r}_2)\hat{\mathbf{p}}_2] \tag{40}$$

and

$$\hat{\mu}(\mathbf{x})=\frac{\hbar\mu_d}{m_p}[\hat{\mathbf{S}}_1\delta^3(\mathbf{x}-\mathbf{r}_1)+\hat{\mathbf{S}}_2\delta^3(\mathbf{x}-\mathbf{r}_2)], \tag{41}$$

respectively, where $\hat{\mathbf{p}}_i$ and $\hat{\mathbf{S}}_i$ are the momentum and spin operators for deuteron i. It follows that in the center-of-mass frame ($\mathbf{r}_1=-\mathbf{r}_2=\mathbf{r}/2$), the convection and magnetization pieces of the various transverse multipole operators reduce to

$$\hat{T}^{\mathrm{el},c}_{J\lambda}(q)=-\frac{4i\hbar}{qm_d}\,P_J^{+}\nabla_{\mathbf{r}}\times[j_J(qr/2)\mathbf{Y}^{\lambda}_{JJ1}(\hat{\mathbf{r}})]\cdot\nabla_{\mathbf{r}}, \tag{42}$$

$$\hat{T}^{\mathrm{el},m}_{J\lambda}(q)=\frac{4\mu_d\hbar}{qm_p}[\hat{\mathbf{S}}_1+(-1)^J\hat{\mathbf{S}}_2]\cdot\nabla_{\mathbf{r}}\times\{\nabla_{\mathbf{r}}[j_J(qr/2)\mathbf{Y}^{\lambda}_{JJ1}(\hat{\mathbf{r}})]\}$$

$$=\frac{\mu_d\hbar q}{m_p}[\hat{\mathbf{S}}_1+(-1)^J\hat{\mathbf{S}}_2]\cdot[j_J(qr/2)\mathbf{Y}^{\lambda}_{JJ1}(\hat{\mathbf{r}})], \tag{43}$$

$$\hat{T}^{\mathrm{mag},c}_{J\lambda}(q)=-\frac{2i\hbar}{m_d}\,P_J^{-}j_J(qr/2)\hat{\mathbf{Y}}^{\lambda}_{JJ1}(\hat{\mathbf{r}})\cdot\nabla_{\mathbf{r}}, \tag{44}$$

and

$$\hat{T}^{\mathrm{mag},m}_{J\lambda}(q)=\frac{2\mu_d\hbar}{m_p}[\hat{\mathbf{S}}_1-(-1)^J\hat{\mathbf{S}}_2]\cdot\nabla_{\mathbf{r}}\times[j_J(qr/2)\mathbf{Y}^{\lambda}_{JJ1}(\hat{\mathbf{r}})], \tag{45}$$

where $P_J^{\pm}\equiv[1\pm(-1)^J]/2$ projects out even or odd values of J, respectively. As is well known it is important to replace the convection current part of the transverse electric operator by a form which has Siegert's theorem built in. Thus we use in place of Eq. (42) the form

$$\hat{T}^{\mathrm{el},c}_{J\lambda}(q)=2\left(\frac{\epsilon_i-\epsilon_f}{\hbar\omega}\right)\sqrt{\frac{J+1}{J}}\left[j_J(qr/2)-\left(\frac{1}{2}qr\right)\frac{1}{J+1}j_{J+1}(qr/2)\right]Y_{J\lambda}(\hat{\mathbf{r}})\hat{\rho}(\mathbf{r})$$
$$+\frac{1}{\sqrt{J(J+1)}}\frac{\hbar q}{m_d}\left[rj_J(qr/2)\frac{d}{dr}+\frac{q}{4(2J+1)}[(3+J)rj_{J-1}(qr/2)-(J-2)rj_{J+1}(qr/2)]\right]Y_{J\lambda}(\hat{\mathbf{r}}) \tag{46}$$

where

$$\hat{\rho}(\mathbf{x})=\delta^3(\mathbf{x}-\mathbf{r}_1)+\delta^3(\mathbf{x}-\mathbf{r}_2). \tag{47}$$

We write the ground state as

$$|0^+\rangle=\sum_L\alpha_L R_L(r)\left[Y_L(\hat{\mathbf{r}})\otimes[\chi_1^{(1)}\otimes\chi_1^{(2)}]_L\right]_{00}, \tag{48}$$

where $R_L(r)$ is normalized to unity and $\alpha_0=\cos\alpha$ and $\alpha_2=\sin\alpha$. The final scattering state is decomposed in the usual fashion as

$$|JMLS\rangle=R_{LS}(kr)\left[Y_L(\hat{\mathbf{r}})\otimes[\chi_1^{(1)}\otimes\chi_1^{(2)}]_S\right]_{JM}. \tag{49}$$

It is then straightforward to show that the various reduced multipole matrix elements are given by

$$\langle JLS||\hat{T}_J^{\text{el},c}(q)||0^+\rangle = \frac{2\alpha_0}{\sqrt{4\pi}} P_J^+ P_L^+ P_S^+ \hat{J}\hat{L} \begin{pmatrix} J & S & L \\ 0 & 0 & 0 \end{pmatrix} \int_0^\infty r^2 dr R_{LS}^*(kr)$$
$$\times \left\{ \left(\frac{\epsilon_i - \epsilon_f}{\hbar\omega} \right) \sqrt{\frac{J+1}{J}} \left[j_J(qr/2) - \left(\frac{1}{2} qr \right) \frac{1}{J+1} j_{J+1}(qr/2) \right] R_0(r) \right.$$
$$+ \frac{\hbar q}{2m_d} \frac{1}{\sqrt{J(J+1)}} \left[r j_J(qr/2) \frac{dR_0(r)}{dr} + \frac{qr}{4(2J+1)} [(3+J) j_{J-1}(qr/2) \right.$$
$$\left. \left. - (J-2) j_{J+1}(qr/2)] R_0(r) \right] \right\}, \tag{50}$$

$$\langle JLS||\hat{T}_J^{\text{el},m}(q)||0^+\rangle = \frac{2\sqrt{6}\mu_d \hbar q}{m_p} \frac{1}{\sqrt{4\pi}} \hat{J}\hat{L} \begin{pmatrix} J & S & L \\ 1 & -1 & 0 \end{pmatrix} \int_0^\infty r^2 dr R_{LS}^*(kr) j_J(x)$$
$$\times \left\{ -\frac{1}{2} P_J^+ P_L^+ P_S^+ \delta_{S2} \alpha_2 R_2(r) + \frac{1}{3} P_J^- P_L^- P_S^- \delta_{S1} \left(\sqrt{2}\alpha_0 R_0(r) - \frac{1}{2} \alpha_2 R_2(r) \right) \right\}, \tag{51}$$

$$\langle JLS||\hat{T}_J^{\text{mag},c}(q)||0^+\rangle = -\frac{i\hbar q}{m_d} \frac{1}{\sqrt{4\pi}} P_J^- P_L^+ P_S^+ \hat{J}\hat{L} \alpha_S \sqrt{S(S+1)} \begin{pmatrix} J & S & L \\ 1 & -1 & 0 \end{pmatrix} \int_0^\infty r^2 dr R_{LS}^*(kr) \frac{j_J(x)}{x} R_S(r), \tag{52}$$

and

$$\langle JLS||\hat{T}_J^{\text{mag},m}(q)||0^+\rangle = \frac{2i\sqrt{6}\mu_d \hbar q}{m_p} \frac{1}{\sqrt{4\pi}} \hat{J}\hat{L} \int_0^\infty r^2 dr R_{LS}^*(kr) \left\{ \frac{1}{3} P_J^+ P_L^- P_S^- \sqrt{J(J+1)} \begin{pmatrix} J & S & L \\ 0 & 0 & 0 \end{pmatrix} \frac{j_J(x)}{x} \right.$$
$$\times \delta_{S1} \left(\alpha_0 R_0(r) + \frac{1}{\sqrt{2}} \alpha_2 R_2(r) \right) + \begin{pmatrix} J & S & L \\ 1 & -1 & 0 \end{pmatrix} \frac{[x j_J(x)]'}{x} \left[P_J^- P_L^+ P_S^+ \frac{1}{2} \delta_{S2} \alpha_2 R_2(r) \right.$$
$$\left. \left. + P_J^+ P_L^- P_S^- \frac{1}{6} \delta_{S1} [\alpha_2 R_2(r) - 2\sqrt{2}\alpha_0 R_0(r)] \right] \right\}, \tag{53}$$

where $x = qr/2$ and where we have used the fact that parity conservation requires P_{J+L}^+ for the electric (and also Coulomb) matrix elements and P_{J+L}^- for the magnetic ones in order to project out the appropriate values for J, L, and S. In these calculations we have included multipoles up to and including $J=4$.

IV. RESULTS AND DISCUSSION

We have investigated a range of observables, polarized and unpolarized, for the photodisintegration of ^{4}He into two deuterons. The object was to assess which, if any, of the photon polarization observables might be useful for studying α-particle ground state properties such as the D wave. In our model the "D-wave properties" are accessed by the D-wave amplitude $\sin(\alpha)$. The effect of reversing the sign of α will be discussed in specific cases. Our view is that if an observable is to be useful in this respect then it must depend mainly on that effect and not on final state interactions (FSI's). Here when we say the FSI effect is of the same size as the D-wave effect we mean that the difference in the observable computed with and without FSI's is the same as the difference in that observable for mixing angles α of 18.4° and 26.6° (P_D = 10% and 20%).[2] For example, all the vector observables p_r and p_r' are extremely sensitive to final state interactions since they are all proportional to the purely imaginary amplitudes $A_{\lambda',\lambda}(1M,k)$. These quantities are only nonvanishing if there are final state interactions. This effect is clearly seen [11] by the disparity in the predictions for A_y ($=p_y$) given by various models. For this reason we will not discuss the vector observables further but turn our attention to the tensor observables. To get a better understanding of the problem we first show in Fig. 1 the FSI and D-wave effects on the single polarization observables at E_γ = 50 MeV. One sees that FSI effects are rather large with the exception of P_{yz} at forward and backward angles. In particular P_{zz} and P_{yy} exhibit a rather strong FSI influence. It is interesting to note that they correspond to T_{20} and A_{yy}, which were measured in [11]. Two observables not shown in Fig. 1 are P_{xx} and P_{xz}. This is because, as can be seen from

[2]Recent calculations of the ^{4}He ground state give a P_D within this range [21].

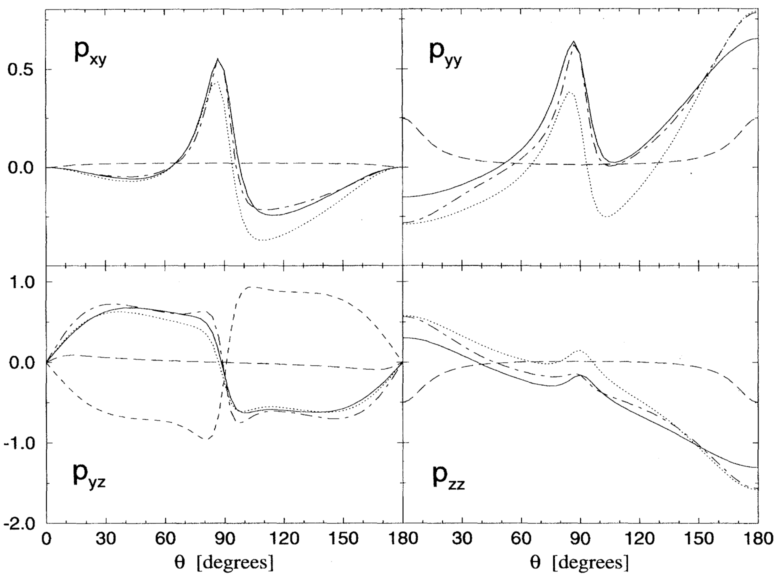

FIG. 1. The observables p_{xy} ($\phi=45°$), p_{yy} ($\phi=0°$), p_{yz} ($\phi=90°$), and p_{zz} ($\phi=0°$) with various ^{4}He D-wave probabilities at $E_\gamma^{\rm lab}=50$ MeV: 0% (long dashed), 10% (dash dotted), 20% (solid), and 20% but opposite sign for the D wave (short dashed) only shown for p_{yz}. The plane wave impulse approximation result with $P_D=20\%$ (dotted) is also depicted.

Eqs. (29) and (31), P_{xx} is very similar to P_{yy} while P_{xz} is essentially identical to P_{yz}. Figure 2 shows that the situation is somewhat similar for double polarization observables. There are, however, interesting features to the observables P_{xz}, P_{yz}, and their primed counterparts. One notes that (i) they basically change sign with the sign of the D-wave amplitude and that (ii) the rise with increasing α is very rapid up to about $P_D=10\%$; in fact $P_D=1\%$ gives about one-half of the effect of $P_D=10\%$. The change of sign arises from that fact that these observables arise mainly from interference between S-wave amplitudes and purely D-wave amplitudes. In fact a fairly good description of the effect is obtained by retaining only the dominantly S-wave (202) $E2$ amplitude and the purely D-wave (221) $M1$ amplitude. The rapid rise of the effect with α can be understood as follows. First we note that in our model the differential cross section depends only weakly on interference between S- and D-wave amplitudes. Thus it has the approximate form

$$\frac{d\sigma}{d\Omega}=A(\theta)\cos^2(\alpha)+B(\theta)\sin^2(\alpha)$$

and hence the observables P_{xz}, P_{yz}, P'_{xz}, and P'_{yz} have the approximate α dependence

$$\frac{\sin(\alpha)\cos(\alpha)}{A\cos^2(\alpha)+B\sin^2(\alpha)}.$$

This form coupled with the observation that for angles θ not near to 0, 90°, or 180° the coefficient $B(\theta)$ tends to be much larger than $A(\theta)$ explains both the rapid rise and saturation of the observables in the P_D range considered here.

From Fig. 3 it appears that the differential cross section at forward or backward angles is extremely sensitive to D-wave effects. Although this is true the differential cross section at these angles is also very sensitive to FSI's. We demonstrate this by plotting in Fig. 4 the total cross section for three values of P_D with the $P_D=20\%$ curve plotted also for plane wave final states. The differences in the total cross sections for the various D-wave probabilities just reflect the differences seen in Fig. 3 at forward and backward angles. One can readily understand the reasons for the strong sensitivity of the differential cross section to P_D by considering only $E1$, $M1$, $E2$, and $M2$ radiation. If the ground state were a pure S wave then there would only be transitions to the (111), (202), and (112) states by $E1$, $E2$, and $M2$ radiation, respectively. Of these transitions, and for the energies

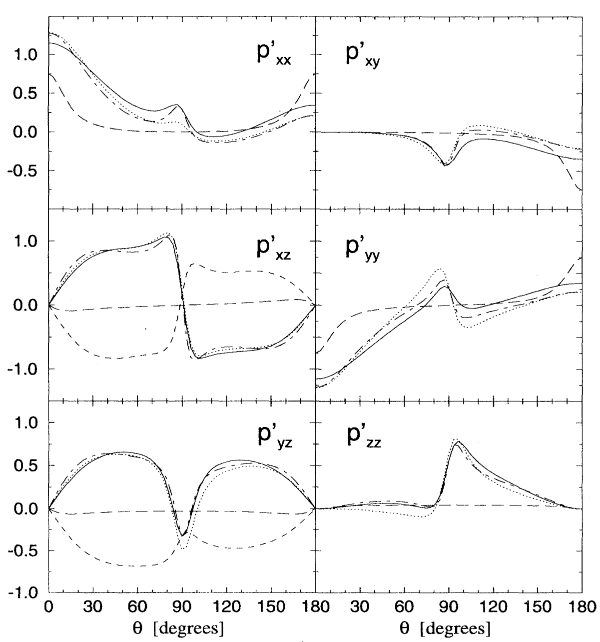

FIG. 2. The photon polarization observables p'_{xx} ($\phi=0°$), p'_{xy} ($\phi=22.5°$), p'_{xz} ($\phi=0°$), p'_{yy} ($\phi=0°$), p'_{yz} ($\phi=45°$), and p'_{zz} ($\phi=0°$) with various ^{4}He D-wave probabilities at $E_\gamma^{\rm lab}=50$ MeV. Notation as in Fig. 1.

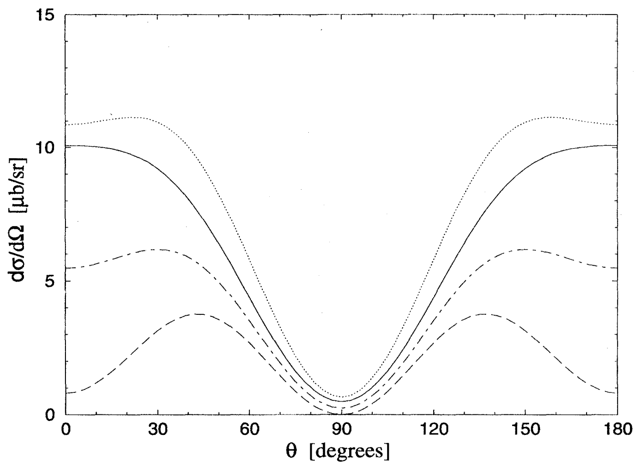

FIG. 3. The differential cross section for ^{4}He$(\gamma,d)^2$H with various ^{4}He D-wave probabilities at $E_\gamma^{\rm lab}=50$ MeV. Notation as in Fig. 1.

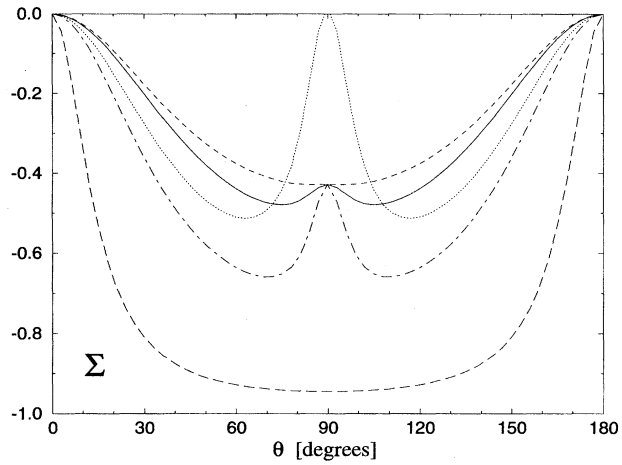

FIG. 5. The photon asymmetry in ^{4}He$(\vec{\gamma},d)^2$H with various ^{4}He D-wave probabilities at $E_\gamma^{\rm lab}=50$ MeV. Notation as in Fig. 1.

we consider here, the $E2$ matrix element is the largest. However, that $E2$ transition has an angular distribution that varies as $\cos^2(\theta)\sin^2(\theta)$ and hence vanishes at forward and backward angles. Thus the forwards-backwards cross section in the case of an S-wave ground state only picks up strength from the relatively small $E1$ (spin flip) and $M2$ transitions. The situation changes radically when we allow for a D-wave component in the ground state. This component then allows an $M1$ transition to the (221) state and $E2$ transitions to the (022), (222), and (422) states. All of these transitions contribute at 0 and 180° and, at least in our model, the $M1$ transition is as strong as the $E2$ transition to the (202) in the energy range $<E_\gamma<150$ MeV. This is also the reason for the large B/A ratio described in the previous paragraph.

In Fig. 5 is plotted the angular distribution of the photon asymmetry Σ for $E_\gamma=50$ MeV. Here one notices a strong dependence on P_D but not on the sign of the D-wave amplitude. The reasons for this are partly given by the discussion in the previous paragraph. That is, the preponderance of matrix elements contributing to either the differential cross section or the asymmetry are those depending on the square of the D-wave amplitude. Thus both quantities are sensitive to P_D and rather insensitive to the sign of the D-wave amplitude. In addition the figure shows that the FSI effect is small except at angles θ near to 90°. The sensitivity to FSI's near 90° is not a serious problem since the cross section is a minimum at that point. The general insensitivity to FSI's occurs because they appear to affect f_{00} and f'_{00} similarly so that their effects "cancel out" in the photon asymmetry. The same results hold for $E_\gamma=100$ MeV. Thus the photon asymmetry appears, on the basis of this calculation, to be strongly dependent on the D-wave content and relatively free of FSI effects.

Concerning the effect of the higher multipoles ($E3$, $M3$, $E4$, $M4$) we find for all observables only negligible contri-

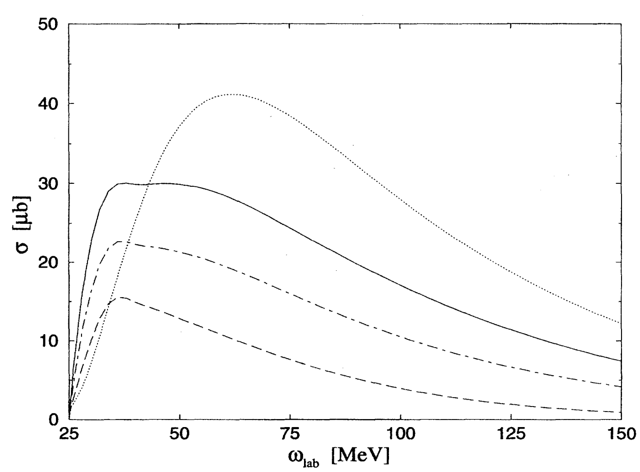

FIG. 4. The total cross section for ^{4}He$(\gamma,d)^2$H with various ^{4}He D-wave probabilities at $E_\gamma^{\rm lab}=50$ MeV. Notation as in Fig. 1.

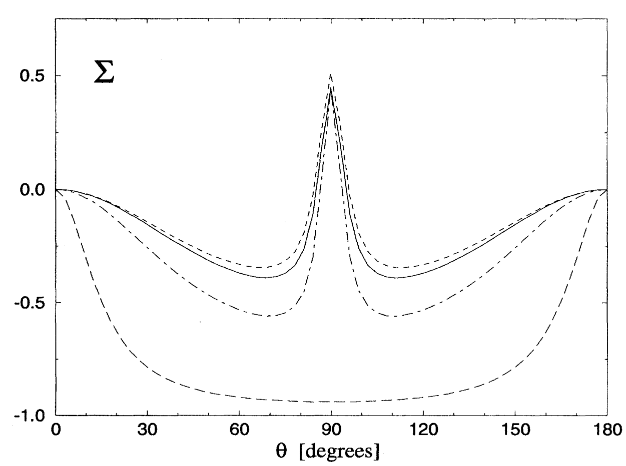

FIG. 6. The photon asymmetry in ^{4}He$(\vec{\gamma},d)^2$H with various ^{4}He D-wave probabilities at $E_\gamma^{\rm lab}=100$ MeV. Notation as in Fig. 1, but here the short dashed curve represents the $P_D=20\%$ result with $E1$, $M1$, $E2$, and $M2$ transitions only.

butions at E_γ = 50 MeV and rather small contributions at 100 MeV. Even at E_γ = 150 MeV there are a number of observables where the higher multipoles can be safely neglected. In fact it is the differential cross section and the γ asymmetry which appear to be most sensitive to the multipole content, although not severely. For example, we plot in Fig. 6 the γ asymmetry at 100 MeV. The P_D=20% curve is calculated first with all multipoles up to and including $J=2$ and then by adding all other multipoles up to and including $J=4$. One observes only very minimal effects. However, we have found that it is important to include the (422) $E2$ matrix element.

In this paper we have set up a formalism for discussing polarization observables in the ^{4}He($\vec{\gamma},\vec{d}$)^{2}H reaction. In addition, on the basis of a simple potential model we suggest that the photon-asymmetry Σ appears to be the most reasonable observable for studying ground state properties. If this can now be corroborated by a microscopic calculation such as the multichannel resonating group calculation of [7] a strong case could be made for doing the experiments.

ACKNOWLEDGMENTS

H.M.H. acknowledges the support of the Deutsche Forschungsgemeinschaft and the BMBF. The work of E.L.T. is supported by the National Science and Engineering Research Council of Canada and the Department of Physics, University of Trento. In addition the authors wish to thank the European Centre for Theoretical Studies in Nuclear Physics and Related Areas (Trento) for providing a stimulating atmosphere for collaborative research.

[1] F.J.W. Wilkinson III and F.E. Cecil, Phys. Rev. C **31**, 2036 (1985).
[2] C.A. Barnes, K.H. Chang, T.R. Donoghue, and C. Rolfs, Phys. Lett. B **197**, 315 (1987).
[3] B.H. Flowers and F. Mandl, Proc. R. Soc. London Ser. A **206**, 131 (1951).
[4] H.R. Weller and D.R. Lehman, Annu. Rev. Nucl. Part. Sci. **38**, 563 (1988).
[5] J. Piekarewicz and S.E. Koonin, Phys. Rev. C **36**, 875 (1987).
[6] G. Blüge, H.J. Assenbaum, and K. Langanke, Phys. Rev. C **36**, 21 (1987).
[7] B. Wachter, T. Mertelmeier, and H.M. Hofmann, Phys. Lett. B **200**, 246 (1988).
[8] H.R. Weller, P. Colby, N.R. Roberson, and D.R. Tilley, Phys. Rev. Lett. **53**, 1325 (1984).
[9] H.R. Weller, P. Colby, J. Langenbrunner, Z.D. Huang, D.R. Tilley, F.D. Santos, A. Arriaga, and A.M. Eiro, Phys. Rev. C **34**, 32 (1986).
[10] J.L. Langenbrunner, G. Feldman, H.R. Weller, D.R. Tilley, B. Wachter, T. Mertelmeier, and H.M. Hofmann, Phys. Rev. C **38**, 565 (1988).
[11] R.M. Whitton, H.R. Weller, E. Hayward, W.R. Dodge, and S.E. Kuhn, Phys. Rev. C **48**, 2355 (1993).
[12] S. Mellema, T.R. Wang, and W. Haeberli, Phys. Lett. **166B**, 282 (1986).
[13] S. Mellema, T.R. Wang, and W. Haeberli, Phys. Rev. C **34**, 2043 (1986).
[14] J.A. Tostevin, Phys. Rev. C **34**, 1497 (1986).
[15] R.G. Seyler and H.R. Weller, Phys. Rev. C **20**, 453 (1979).
[16] T.A. Welton, in *Fast Neutron Physics*, edited by J. B. Marion and J. L. Fowler (Interscience, New York, 1963).
[17] A.R. Edmonds, *Angular Momentum Theory in Quantum Mechanics* (Princeton University Press, Princeton, 1952).
[18] T. deForest and J.D. Walecka, Adv. Phys. **15**, 1 (1966).
[19] G.G. Ohlsen, Rep. Prog. Phys. **35**, 717 (1972).
[20] H.R. Weller, Nucl. Phys. **A508**, 273 (1990).
[21] J. Carlson, Phys. Rev. C **38**, 1879 (1988).
[22] A. Arriaga, V.R. Pandharipande, and R. Schiavilla, Phys. Rev. C **43**, 983 (1991).